Reaction Chemistry & Engineering

ROYAL SOCIETY OF CHEMISTRY

PAPER

View Article Online
View Journal | View Issue

Cite this: *React. Chem. Eng.*, 2020, 5, 183

Catalytic methanation of CO_2 in biogas: experimental results from a reactor at full scale†

Christian Dannesboe, *[a] John Bøgild Hansen[b] and Ib Johannsen[a]

Received 27th August 2019,
Accepted 25th November 2019

DOI: 10.1039/c9re00351g

rsc.li/reaction-engineering

In a future energy scenario without fossil fuels carbon from renewable biomass will be a limited resource. Full carbon utilization through catalytic methanation of CO_2 in biogas appears to be a low hanging fruit. However, concerns on catalyst cost and wear, elaborate reactor cooling requirements and significant costs related to post-treatment are reported from theoretical studies and early demonstration plants. In this study, we show how a full scale methanation reactor can be operated under favourable process conditions for 1000 hours without complications. We find that operating the reactor at a sub-stoichiometric ratio of 3.9 is optimal in order to deliver pipeline quality gas. The temperature profile shows how start and stop can be performed within minutes, and the combined studies presented are a breakthrough in direct catalytic upgrading of biogas ready for industrial scale implementation.

Introduction

Today, electricity from fossil resources struggle to compete with cheap electrical power harvested in efficient solar and wind energy-parks. Consequently, the production of electricity from renewable sources is expanding rapidly. Within the EU, 85% of the new electricity-generating capacity utilize renewable resources. Moreover, the majority of the decommissioned capacity is conventional facilities.[1] Although these changes provide cheap renewable electricity, the imbalance between production and demand imposes a significant supply challenge. The ability to store energy for hours and days may be considered using existing battery technology,[2] but the requirements of future energy solutions will rely on massive storage facilities to cope with imbalances lasting weeks, months and even seasonal variation. Hence, there is a need to develop other types of storage technologies to aid further implementation of renewable energy. Power to gas is based on the conversion of electricity to hydrogen *via* electrolysis and can enable chemical storage of energy. Hydrogen is, however, not the ideal candidate for a storage application, as significant compression (>100 bar) is required to reach a moderate energy density.[3] Natural gas (methane) is a very effective and fully established energy carrier in all parts of the world. The energy density of methane is three times higher than hydrogen, and facilities for transport and storage are widespread. Converting hydrogen to methane can be done with methanation[4] (eqn (1)), enabling storage of renewable energy as methane.

$$4H_{2(g)} + CO_{2(g)} \rightleftarrows CH_{4(g)} + 2H_2O_{(g)} \quad \Delta H_{300°C} = -165 \text{ kJ mol}^{-1} \quad (1)$$

Biogas produced from biomass (*i.e.* manure or other agricultural side streams) produce a methane-rich gas. As only around 60% is methane, the main contaminant CO_2 (40%) is normally discarded through a separation process and the remaining methane can be exported using the existing gas grid. The swap to renewable gas is straightforward and a significant replacement of natural gas by renewable methane is observed in countries like Denmark, Sweden, Germany and the Netherlands. In July 2018 Denmark reported a record 18% of the national gas demand supplied from biogas plants.[5] Although methanation of CO_2 in biogas enable full utilization of renewable carbon, this practice is not common. Studies of economic feasibility highlight how renewable methane from biogas have difficulties in competing with the very low price of natural gas, given the limited political initiatives to enforce significant fossil taxation.[6] In addition, hydrogen from renewable resources is required, and the low electrical conversion efficiency of alkaline and proton-exchange-membrane electrolysis units (50–65% on a lower heating value basis[7]) makes renewable methane production *via* methanation costly. Even though significant improvements have been achieved, the cost of hydrogen remains the single most important factor affecting methanation plants.[8–10]

[a] *Department of Engineering, Aarhus University, Hangøvej 2, DK-8200 Aarhus N, Denmark. E-mail: chda@ase.au.dk, ibj@eng.au.dk*
[b] *Haldor Topsøe A/S, Nymøllevej 55, DK-2800 Kongens Lyngby, Denmark. E-mail: jbh@topsoe.com*

† Electronic supplementary information (ESI) available. See DOI: 10.1039/c9re00351g

Numerous reviews of CO_2 methanation technology highlight several significant costs and process constraints to reach full implementation at an industrial scale. Efficient cooling of a fixed bed methanation reactor is required to avoid catalyst deactivation (thermal sintering) in the reactor hotspot.[11–14] This leads to a reactor design with multiple cooling loops including expensive hot oil or molten salt systems.[9,14,15] Alternatively, several reactors in series or a large and costly recycle loop is required.[14] Catalyst deactivation by carbon formation is also a thoroughly documented problem.[11,15,16] In the specific case of direct methanation of CO_2 in biogas, potential methane cracking is especially relevant. Carbon formation has been reported when operating the methanation reaction below a stoichiometric ratio of 4.[9,11,12,17] Several studies on the quality of the produced gas conclude inadequate export quality from a single pass reactor. Two separate reactors, with intermediate water removal, will be needed to achieve the required conversion of CO_2 and H_2.[9,10,13] Conversion is favoured by a low reactor temperature (*i.e.* 250–300 °C). However, low catalyst activity at this process temperature limits conversion by kinetic constraints.[8,13,17] Insufficient conversion leads to costly removal of reactants downstream (*i.e.* membrane purification) to achieve >97% CH_4 content.[9,10,18]

The concerns above have resulted in expensive and overcautious design of CO_2 methanation plants. In this work, we show how most of these concerns, although thoroughly documented, can be attributed to misleading guidelines adapted from the experience of CO methanation and recommendations when using catalysts with moderate resistance to thermal sintering. We report the experimental data from a full-scale methanation reactor for direct catalytic methanation of CO_2 in biogas. Using raw biogas as feed, the reactor is operated for 1000 hours and prove how state-of-the-art CO_2 methanation technology offer pipeline grade natural gas without the need for downstream removal of unreacted H_2 and CO_2. Additionally, efficient cooling is obtained using a simple boiling water reactor design.

Experimental

The methanation reactor presented here is part of a combined electrolysis–methanation system using solid oxide electrolysis cells (SOEC). The idea of utilizing synergies between SOEC and direct catalytic methanation of CO_2 in biogas was first suggested at the European Fuel Cell conference in Rome, 2001.[19] Similar design ideas including catalytic methanation and biogas quickly followed in the years to come.[10,20,21] In essence, the pilot plant consists of a biogas pretreatment section, a full-scale methanation reactor and a water separation/gas drying section. The treatment steps are shown in Fig. 1.

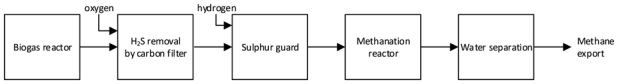

Fig. 1 Block diagram of the steps required when upgrading raw biogas to methane.

Biogas pretreatment

Raw biogas was delivered directly from the biogas reactor at AU Foulum. Bulk removal of H_2S was done by activated carbon. The potassium iodine impregnated alkaline activated carbon used was SOLCARB® KS3 (Chemviron Carbon, Lancashire, United Kingdom). This removes hydrogen sulfide from ~1000 ppm to ~1 ppm, but sulfur species like carbondisulfide, dimethylsulfide and carbonylsulfide will leak through.[22] A final sulfur guard removes all residual sulfur compounds to ppb level (zinc oxide absorbent, HTZ-51, Haldor Topsøe A/S, Kgs. Lyngby, Denmark). The biogas is produced exclusively from caw manure and straw. Contaminants like aromatic compounds or terpenes are not observed as a problem from this feedstock. A detailed study of the biogas pretreatment section can be found in literature.[22] The biogas flow is measured using a Coriolis flowmeter (Proline Promass 80A, Endress+Hauser AG, Switzerland) and controlled using a flow-valve (RC200, Badger Meter Europa GmbH, Germany). Hydrogen flow is controlled by a mass flow controller (EL-FLOW, Bronkhorst High-Tech B.V., Netherlands). Mixing of biogas and hydrogen is ratio-controlled with the hydrogen flow fixed.

Methanation reactor

The processing capacity of the methanation reactor was chosen to be 10 $Nm^3\ h^{-1}$ biogas. This capacity was selected as it represents the smallest possible full-scale design of a multi-tube packed bed reactor. The reactor is a double pass design, *i.e.* the smallest possible multi tube reactor consist of only two tubes (Fig. 2). Upscaling of this reactor to obtain higher processing capacity would only affect the number of tubes as gas hour space velocity (GHSV), linear velocity and tube dimensions remain unchanged. The packed bed height is 2.3 m. Boiling water is used as the reactor cooling strategy. Pressurizing the cooling water to 65 bar keeps the boiling

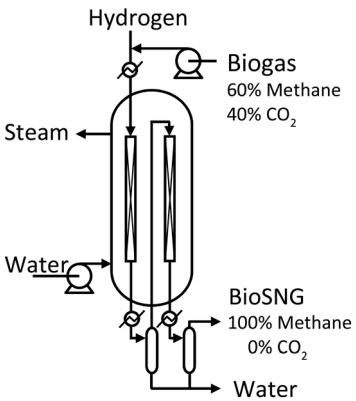

Fig. 2 Design of the double pass, packed bed, boiling water reactor with condensate removal after the first pass. Included from earlier work.[23]

point at 280 °C (the desired reactor temperature[23]). The specific dimensions of the two reactor tubes is proprietary information of Haldor Topsøe A/S.

The loaded methanation catalyst is HT-25442. This is a cylindrical shaped Ni/Al_2O_3 based methanation catalyst specifically designed to withstand long term operation at up to 700 °C like the MCR-2 catalyst described in literature.[24,25] A reactor exit pressure of 20 barg is maintained by a pressure valve (RC200, Badger Meter Europa GmbH, Germany).

A detailed temperature profile through the first reactor tube allows monitoring catalyst performance during startup and shutdown as well as hotspot migration (an indicator of catalyst deactivation). The temperature profile is recorded using a multipoint thermocouple with 3 cm spacing between the probes (Thermo Electric Instrumentation B.V., Netherlands). The reactor tube has a length of 2.4 m and is equipped with 16 temperature probes to provide a full profile.

After the first pass, the produced water is removed by condensation before the gas is passed through the second reactor tube. This double pass strategy ensures a methane content/Wobbe index within the specifications of natural gas.[23]

Actual gas composition is measured by a gas chromatograph (Micro GC 490, Agilent Technologies, United States) equipped with two channels (MS5A and PPQ columns) and a thermal conductivity detector allowing analysis of hydrogen, nitrogen, methane, carbon monoxide and carbon dioxide. Using automatic sampling, the GC performs online analysis, but some delay is expected due to machine processing time and the physical distance the sample has to travel to the GC.

Comparison of simulation and methanation data

To compare the theoretical equilibrium of the methanation reaction with data from the methanation reactor, a simulation study was performed using Aspen Plus software (Aspen Tech, Unites States). The simulation used the Gibbs reactor. Water removal by condensation was included in the model by using the flash drum unit. Both reactor tubes and both condensation steps were included to allow direct comparison of the gas composition. In the model, a biogas composition of 60% methane and 40% CO_2 was used. The equation of state model Soave–Redlich–Kwong was the basis of the calculations. The effect of changing the CO_2 to H_2 ratio was investigated (stoichiometric ratio is 1 : 4). H_2 surplus was adjusted from 3.75 to 4.15 in the model. The experimental data from the methanation reactor was obtained in a similar way by adjusting the ratio between CO_2 and H_2. The ratio-change was performed during a five-hour period using a ramp. The change was slow to minimize the delay-effect from the sample processing time.

Results and discussion

Temperature profile of the methanation reactor

During the test period, the methanation reactor was in operation for 1000 hours in total. The temperature profile through the first reactor tube (Fig. 3) reveals an extremely rapid temperature increase, a temperature hotspot just below 680 °C and very efficient cooling within only 0.5 m. The exothermal methanation reaction is close to complete within the first 0.5 m of the reactor tube. Hotspot migration down the reactor tube is not observed during 1000 h of operation. The data indicate no catalyst deactivation. Consequently, the biogas pretreatment must be excellent. The observed differences are expected to arise from small flow variations between the test runs.

Temperature readings from startup (Fig. 4a) show how the methanation reaction is engaged within minutes. Fig. 4a also show how steady state operation with respect to the temperature profile is obtained after 25 minutes, and how shutdown can be performed within minutes (Fig. 4b). In the first minutes of the startup, the exothermal reaction heats the reactor tubes and catalyst mass to the final steady state temperature. The result is a slightly increased cooling capacity until steady state is obtained. Theoretically, this will result in a satisfactory gas quality very rapidly (before the temperature probes stabilize), but this has not yet been confirmed experimentally. Startup and shutdown data at every thermocouple position are available as supplementary material (Fig. SI 1 and SI 2†).

Investigation of the chemical equilibrium

Simulation studies of the ratio between H_2 and CO_2 (Fig. 5) confirm how the highest methane content can be obtained at the stoichiometric ratio of 4. Operating near the stoichiometric ratio of 4 produces a gas within the European Norm on natural gas.[26] This allows direct export without downstream removal of H_2 and CO_2. From an operational perspective, the simulations show how a ratio of

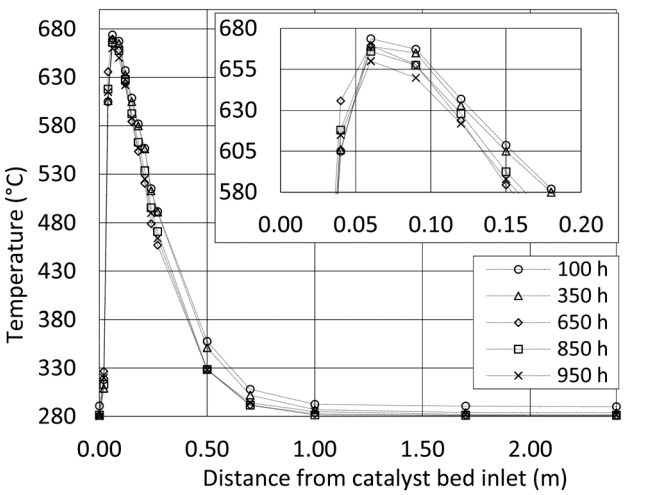

Fig. 3 Temperature profile of the first reactor tube. The profiles show operation after 100 hours (circle), 350 hours (triangle), 650 hours (diamond), 850 hours (square) and 950 hours (cross). Average processing in the period was 5 $Nm^3\ h^{-1}$ biogas and 8 $Nm^3\ h^{-1}$ H_2 at 20 barg with a H_2/CO_2 ratio of 4.

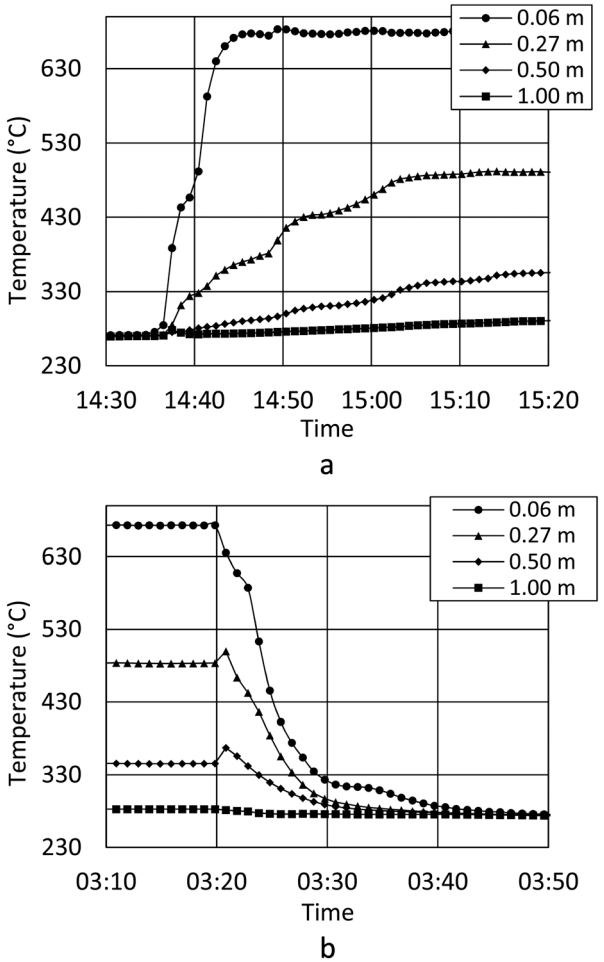

Fig. 4 a Temperature development during startup of the reactor. The distance from catalyst bed inlet is 0.06 m (circle), 0.27 m (triangle), 0.50 m (diamond) and 1.00 m (square). Processing of 9.70 $Nm^3\ h^{-1}$ biogas and 15.9 $Nm^3\ h^{-1}$ H_2 at 20 barg with a H_2/CO_2 ratio of 4.1. b Temperature development during shutdown of the reactor. The distance from catalyst bed inlet is 0.06 m (circle), 0.27 m (triangle), 0.50 m (diamond) and 1.00 m (square). Processing of 9.70 $Nm^3\ h^{-1}$ biogas and 15.9 $Nm^3\ h^{-1}$ H_2 at 20 barg with a H_2/CO_2 ratio of 4.1.

3.9 to 3.95 would be preferred. Each simulation assume full chemical equilibrium is achieved.

Experimental data from the methanation reactor are summarized in Fig. 6 along with simulated values. Above the stoichiometric ratio of 4 (*i.e.* H_2 surplus) the data show excellent agreement with the simulation. Full chemical equilibrium is achieved. Below the stoichiometric ratio (*i.e.* CO_2 surplus), the data clearly deviate from the chemical equilibrium. As the reaction requires four H_2 for every CO_2, the deviation is very clear for hydrogen. At a ratio of 4.00 to 4.05 the experimental data appear noisy. Analysis of methane in this range show values above and below the equilibrium line, and individual measurements show significant variation. This might be explained by unforeseen sudden variation in biogas feed (like start/stop of mixers in the biogas reactor), but the direct course is unknown.

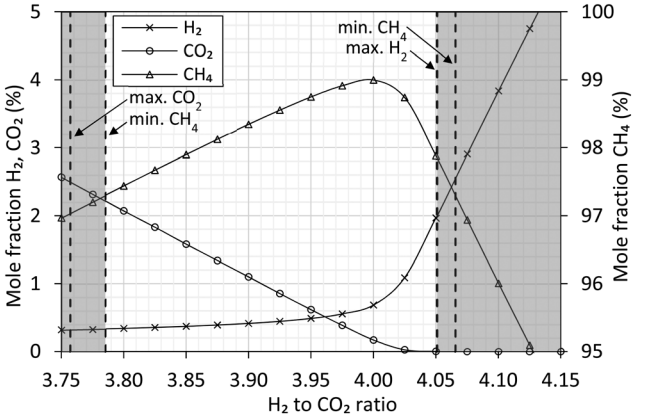

Fig. 5 Aspen Plus simulation at 280 °C, 20 barg of the equilibrium composition between feed and reactants of the methanation reaction (eqn (1)). The feed composition is varied around the stoichiometric ratio of H_2 to CO_2. The gas composition is expressed as molar fraction of H_2 (cross), CO_2 (circle) and CH_4 (triangle). Vertical dashed lines represent the gas specification[26] and indicate the limits allowing direct export of the produced gas.

Performance of the methanation reactor

Results from 1000 hours of production of a full scale methanation reactor for direct conversion of CO_2 in biogas has been presented. The results show how the boiling water reactor offer very efficient cooling of the exothermal methanation reaction. The double pass design with water removal after the first pass ensures a robust solution as the produced gas is in agreement with the European Norm (EN 16726) in a wide operational window (3.8 to 4.05). Analysis confirms a gas quality within the specification of natural gas if the residual moisture is reduced to satisfy the dew point specification. Experimental results confirm how start and stop of the methanation reactor can be achieved in a timescale of minutes (from hot standby). This will be the

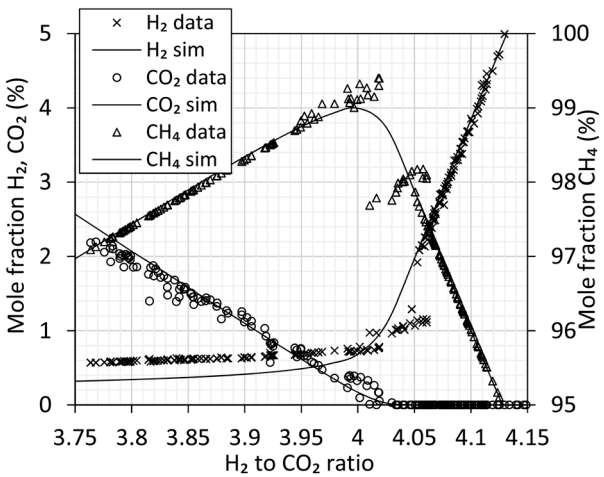

Fig. 6 Analysis of the produced gas using gas chromatography. Gas composition is expressed as molar fraction of H_2 (cross), CO_2 (circle) and CH_4 (triangle). Processing of 7.0 $Nm^3\ h^{-1}$ H_2 at 280 °C, 20 barg. Simulated equilibrium curves from Fig. 5 are included as reference.

requirement if the methanation reactor is combined with an electrolysis unit in future grid stabilization applications. This process flexibility is also confirmed at other pilot facilities.[9,13] As the temperature hotspot in the reactor is steady after 1000 hours, no decrease in catalyst activity was noted. This can only be explained by excellent sulfur removal and a catalyst not predisposed to sintering or carbon formation. The results also point towards a possible final reactor design with shorter tubes of 1 m being sufficient.

Carbon formation below stoichiometric ratio of four

This simulation study finds the optimum H_2 to CO_2 ratio to be 3.9 to 3.95. The result is identical to simulation studies by others.[9] Operating at a ratio below 4 was also previously recommended by a third group,[16] however the proposed guideline from this last study, with a ratio as low as 3.4, is only possible due to a higher allowed CO_2 concentration of 6% at a specific location. Despite these recommendations, recently built demonstration plants have specifically chosen to operate at a ratio above 4, due to the risk of carbon formation when operating at a sub-stoichiometric ratio.[9,13] This guideline originates from the experiences of CO methanation, where carbon formation *via* the Boudouard reaction can be a significant problem.[11,15,17] A second concern is previous findings of significant carbon deposition at 500–800 °C specifically using Ni/Al_2O_3 catalyst due to methane decomposition.[27] A more recent study using a Ni/CeO_2–ZrO_2 catalyst also observe carbon formation at sub-stoichiometric ratio,[12] whereas other studies of CO_2 methanation[28] observe no carbon formation in any of the spend catalyst samples.

In case of CO methanation, the hotspot temperature shown here (>550 °C, Fig. 3) would require increased pressure and steam addition to ensure the chemical equilibrium would not favor severe carbon formation. However, as CO is not present in the feed gas and as steam is produced by the reaction, carbon formation is not an issue.[17] Past studies of CO and CO_2 methanation have also shown how, although favorable, carbon formation can be suppressed by ensuring the metal crystals on the support are very fine,[29] by sulfur passivation[30] or by adding promoters like CeO_2.[27] The risk of carbon formation from the Boudouard reaction and from methane decomposition at various H/C and O/C ratios can be evaluated using the thermodynamic data from litterature.[31] If the equilibrated gas (with respect to methanation and the water gas shift reaction) shows affinity for carbon formation, graphite precipitation will take place in the form of whiskers with the same dimensions as the nickel crystals in the catalyst. The hotspot temperature in the reactor (Fig. 3) is within the carbon formation region (Fig. 7), calculated using thermodynamic data for graphite formation, but the small nickel crystal size in the catalyst prevents carbon whisker formation and continued operation can be performed without any catalyst deactivation by coking. The guidelines presented here are not new, but knowledge of their existence is often overlooked.

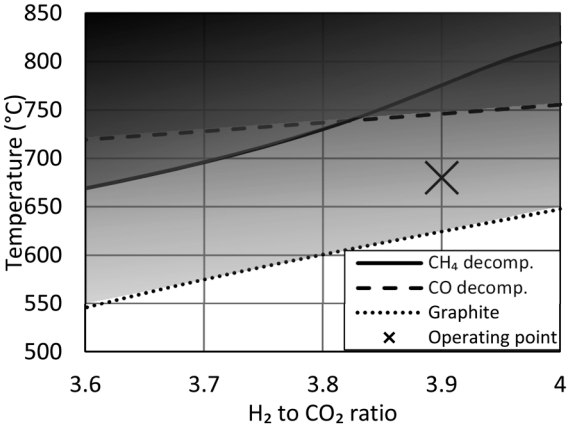

Fig. 7 Carbon limit temperatures indicating risk of graphite precipitation (dotted line) and carbon deposition from decomposition of CH_4 (solid line) or CO (dashed line). Carbon limits calculated using thermodynamic data[31] at 20 barg. The actual hotspot temperature of the reactor (Fig. 3) is marked with an X.

Deviation from chemical equilibrium

The results presented here show how full chemical equilibrium is obtained when operating the CO_2 methanation reaction above the stoichiometric ratio of 4. Satisfactory estimates on gas composition are obtained from simple minimization of Gibbs free energy; even though employing this method means ignoring all kinetic limitations. However, a contradictory observation can also be made from the experimental results presented here. At sub-stoichiometric ratio (Fig. 6), the gas analysis could indicate that complete chemical equilibrium is not obtained. Due to the reaction stoichiometry, this effect is very clear for hydrogen. This could spark renewed considerations into the rate determining step (RDS) of CO_2 methanation. Clarifying the mechanism of CO_2 methanation has been attempted for 100 years (!) and an overwhelming amount of research papers, both experimental and theoretical, have been published. However, still no consensus exists.[15,28,32,33] One of the central questions is whether CO_2 methanation proceeds *via* a CO intermediate[34] or if a direct route[35] *via* formate or carbonate is preferred. Some results[36–38] point towards a direct CO intermediate route, but an intermediate route *via* formate to CO is also possible.[39,40] However, other results indicate no CO intermediate is required.[41,42] A review on the mechanism of CO_2 methanation,[33] note how the formate route (without a CO intermediate) is only observed by research groups using hydrogen levels far above stoichiometric ratio (5 : 1, 9 : 1). At stoichiometric ratio, the methanation of CO_2 will probably proceed *via* a CO intermediate, but several viable routes towards the CO intermediate exists. The intermediate CO has been confirmed at stoichiometric ratio of 4 during CO_2 methanation at 300 °C by *in situ* infrared spectroscopy.[28] The

preferred CO_2 methanation pathway will be a result of catalyst composition, temperature and hydrogen ratio.[33] The CO_2 methanation mechanism may occur *via* parallel routes simultaneously.[40]

The data presented here clearly show how CO_2 methanation can proceed without the sintering and carbon deposition challenges specifically caused by CO in CO methanation. Our results, as also observed by others,[13] show no CO in the final gas. The data presented indicate a change in the methanation reaction occurring at a ratio of 3.95 and could explain how different studies all claiming to operate at the same stoichiometric ratio of ~4 could differ significantly.

Conclusion

Direct methanation of CO_2 in biogas enables full carbon utilization from biomass. When combined with electrolysis, conversion and storage of electricity as natural gas is possible. Large-scale implementation is however restricted by concerns of significant catalyst cost and wear, elaborate reactor cooling requirements and significant costs related to post-treatment of the produced gas. Based on these guidelines, current feasibility studies and demonstration plants highlight the need for further development. In this study, we have shown how full scale methanation of CO_2 in biogas can be performed without complications. We document 1000 hours of operation in process conditions favoring carbon deposition without any catalyst deactivation. Our studies show, that the cautious guidelines on carbon formation, thermal sintering and operation below stoichiometric ratio clearly needs to be revised. Operations around the stoichiometric ratio indicate a change in the mechanism of CO_2 methanation, as the reaction only deviate from chemical equilibrium below the stoichiometric ratio. Experimental results confirm how start and stop can be achieved within minutes.

Further research into improved performance of CO_2 methanation catalyst seems difficult to justify, as current technology outperforms the lifetime of most other plant components. The high efficiency of the catalyst will limit the sales volume and even large-scale biogas plants (1000 $Nm^3 h^{-1}$) barely require more than a typical absolute minimum order of catalyst.

Conflicts of interest

There are no conflicts to declare.

Acknowledgements

This project was made possible by 5.3 mio. € funding from the Danish Energy Technology Development and Demonstration Program (EUDP).

References

1 C. Nissen, F. Meinke-Hubeny, L. Emele, M. Tomescu, A. Das and I. Moorkens, *Renewable energy in Europe 2018*, European Topic Centre for Air Pollution and Climate Change Mitigation, 2019.
2 H. Blanco and A. Faaij, *Renewable Sustainable Energy Rev.*, 2018, **81**, 1049–1086.
3 G. Marbán and T. Valdés-Solís, *Int. J. Hydrogen Energy*, 2007, **32**, 1625–1637.
4 P. Sabatier and J. B. Senderens, *Comptes Rendus Acad. Sci.*, 1902, **Section VI - Chimie**, 514–517.
5 Energinet, *Gasforsyningssikkerhed 2018*, Energinet, 2018.
6 J. D. Jenkins and V. J. Karplus, *Carbon pricing under binding political constraints, Report 1798–7237*, United Nations University, 2016.
7 F. M. Sapountzi, J. M. Gracia, C. J. Weststrate, H. O. A. Fredriksson and J. W. Niemantsverdriet, *Prog. Energy Combust. Sci.*, 2017, **58**, 1–35.
8 M. A. A. Aziz, A. A. Jalil, S. Triwahyono and A. Ahmad, *Green Chem.*, 2015, **17**, 2647–2663.
9 S. Biollaz, A. Calbry-Muzyka, T. Schildhauer, J. Witte and A. Kunz, *Direct Methanation of Biogas*, Paul Scherrer Institut, 2017.
10 L. Wang, M. Pérez-Fortes, H. Madi, S. Diethelm, J. V. Herle and F. Maréchal, *Appl. Energy*, 2018, **211**, 1060–1079.
11 C. H. Bartholomew, *Appl. Catal., A*, 2001, **2012**, 17–60.
12 F. Ocampo, B. Louis, A. Kiennemann and A. C. Roger, *IOP Conf. Ser.: Mater. Sci. Eng.*, 2011, **19**, 012007.
13 M. Gruber, P. Weinbrecht, L. Biffar, S. Harth, D. Trimis, J. Brabandt, O. Posdziech and R. Blumentritt, *Fuel Process. Technol.*, 2018, **181**, 61–74.
14 S. Rönsch, J. Schneider, S. Matthischke, M. Schlüter, M. Götz, J. Lefebvre, P. Prabhakaran and S. Bajohr, *Fuel*, 2016, **166**, 276–296.
15 G. A. Mills and F. W. Steffgen, *Catal. Rev.: Sci. Eng.*, 1974, **8**, 159–210.
16 L. Jurgensen, E. A. Ehimen, J. Born and J. B. Holm-Nielsen, *Bioresour. Technol.*, 2015, **178**, 323–329.
17 J. Gao, Y. Wang, Y. Ping, D. Hu, G. Xu, F. Gu and F. Su, *RSC Adv.*, 2012, **2**, 2358.
18 F. Bauer, C. Hulteberg, T. Persson and D. Tamm, *Biogas upgrading – Review of commercial technologies, Report 270*, Svenskt Gastekniskt Center AB, 2013.
19 J. B. Hansen, C. F. Pedersen, J. U. Nielsen and N. Christiansen, *European Fuel Cell 2011*, Rome, Italy, 2011.
20 *HELMETH*, 2018, p. 36.
21 E. Giglio, A. Lanzini, M. Santarelli and P. Leone, *J. Energy Storage*, 2015, **1**, 22–37.
22 C. Dannesboe, J. B. Hansen and I. Johannsen, accepted for publication in *Biomass Conversion and Biorefinery* (ISSN 2190-6815) as manuscript No. BCAB-D-19-00414R1, 2019.
23 C. Dannesboe, J. B. Nielsen and I. Johannsen, 2019, in preparation.
24 J. R. Rostrup-Nielsen, K. Pedersen and J. Sehested, *Appl. Catal., A*, 2007, **330**, 134–138.
25 T. T. M. Nguyen, L. Wissing and M. S. Skjøth-Rasmussen, *Catal. Today*, 2013, **215**, 233–238.
26 EN 16723-1:2016, European Committee for Standardization, Brussels, CEN Management Center, 2016.
27 S. Wang and G. Q. Lu, *Appl. Catal., B*, 1998, **19**, 267–277.

28 H. Muroyama, Y. Tsuda, T. Asakoshi, H. Masitah, T. Okanishi, T. Matsui and K. Eguchi, *J. Catal.*, 2016, **343**, 178–184.
29 H. Harms, B. Höhlein and A. Skov, *Chem. Ing. Tech.*, 1980, **52**, 504–515.
30 J. R. Rostrup-Nielsen, *Stud. Surf. Sci. Catal.*, 1991, **68C**, 85–101.
31 J. R. Rostrup-Nielsen, *Catalytic Steam Reforming*, Springer-Verlag, 1984.
32 X. Su, J. Xu, B. Liang, H. Duan, B. Hou and Y. Huang, *J. Energy Chem.*, 2016, **25**, 553–565.
33 B. Miao, S. S. K. Ma, X. Wang, H. Su and S. H. Chan, *Catal. Sci. Technol.*, 2016, **6**, 4048–4058.
34 H. A. Bahr, *Gesammelte Abh. Kennt. Kohle*, 1929, **8**, 219.
35 H. Pitcher, *Brennst.-Chem.*, 1943, **24**, 39.
36 I. A. Fischer and A. T. Bell, *J. Catal.*, 1996, **162**, 54–65.
37 C. d. Leitenburg, A. Trovarelli and J. Kaspar, *J. Catal.*, 1997, **166**, 98–107.
38 A. Beuls, C. Swalus, M. Jacquemin, G. Heyen, A. Karelovic and P. Ruiz, *Appl. Catal., A*, 2012, **113–114**, 2–10.
39 F. Solymosi, A. Erdöhelyi and T. Bansagi, *J. Catal.*, 1981, **68**, 371–382.
40 M. Marwood, R. Doepper and A. Renken, *Appl. Catal., A*, 1997, **151**, 223–246.
41 H. Y. Kim, H. M. Lee and J.-N. Park, *J. Phys. Chem. C*, 2010, **114**, 7128–7131.
42 Z. A. Ibraeva, N. V. Nekrasov, B. S. Gudkov, V. I. Yakerson, Z. T. Beisembaeva, E. Z. Golosman and S. L. Kiperman, *Kinet. Catal.*, 1990, **26**, 584–588.